Bayesian Analysis of ODE's: solver optimal accuracy and Bayes factors

Marcos A. Capistrán[a][*], J. Andrés Christen[a][†]and Sophie Donnet[b][‡]

[a]*Centro de Investigación en Matemáticas, Guanajuato, México*;

[b]*INRA, Unité MIA, Equipe MORSE, France.*

10 November 2013

Abstract

In most relevant cases in the Bayesian analysis of ODE inverse problems, a numerical solver needs to be used. Therefore, we cannot work with the exact theoretical posterior distribution but only with an approximate posterior deriving from the error in the numerical solver. To compare a numerical and the theoretical posterior distributions we propose to use Bayes Factors (BF), considering both of them as models for the data at hand. We prove that the theoretical vs a numerical posterior BF tends to 1, in the same order (of the step size used) as the numerical forward map solver does. For higher order solvers (eg. Runge-Kutta) the Bayes Factor is already nearly 1 for step sizes that would take far less computational effort. Considerable CPU time may be saved by using coarser solvers that nevertheless produce practically error free posteriors. Two examples are presented where nearly 90% CPU time is saved while all inference results are identical to using a solver with a much finer time step.

KEYWORD: Inverse Problems; Bayesian Inference; Bayes Factors; Numerical Analysis of ODE's.

1 Introduction

1.1 Context and issues

In a comprehensive review of recent publications on the Bayesian Analysis of Inverse Problems it is clear that there is a consistent growth of interest in the

---

[*]Email: *marcos@cimat.mx*

[†]Corresponding author. Email: *jac@cimat.mx*

[‡]Email: *sophie.donnet@agroparistech.fr*

uncertainty quantification approach provided by the Bayesian paradigm. However, we also notice that some of the potential strength of the Bayesian approach is currently underexploited, namely, 1) prediction, 2) model selection and (let alone) 3) decision making under uncertainty. Recent reviews on the Bayesian Analysis of inverse problems (Mohammad-Djafari, 2006; Kaipio and Fox, 2011; Watzenig and Fox, 2009; Kaipio and Fox, 2011; Woodbury, 2011) do not discuss these former points in detail. We have now access to important theoretical results on the definition of posterior distributions in infinite dimensions and regularity conditions for correct approximate schemes through numerical, finite dimension posteriors (eg. Schwab and Stuart, 2012) that provide a sound theoretical background to the field. There are several applications in the (Bayesian dominated) field of image processing of various kinds (Zhu et al., 2011; Cai et al., 2011; Fall et al., 2011; Chama et al., 2012; Kolehmainen et al., 2007; Nissinen et al., 2011; Kozawa et al., 2012, to mention some recent references), and also we find a whole range of emerging application areas in the Bayesian Analysis of inverse problems (Calvetti et al., 2006; Keats et al., 2010; Cui et al., 2011; Wan and Zabaras, 2011; Hazelton, 2010; Kaipio and Fox, 2011). However, only a handful of publications mentions or uses Bayesian predicting tools, that is, the posterior (predictive) distribution of yet to observe variables (Vehtari and Lampinen, 2000; Somersalo et al., 2003; Kaipio and Fox, 2011; Capistrán et al., 2012), and even less consider formally the model selection and model comparison tools developed in Bayesian statistics. We intend to contribute to the formal and more systematic use of the latter in the context of Inverse Problems.

Predictive power is always a desirable property of mathematical models and inference, beyond parameter estimation, for model parameters that may or may not have straightforward physical meaning. We believe that comparing forward models as *statistical* models is the way to proceed when predictive power is of main interest. The Bayesian model comparison and model averaging tools, in particular pairwise model comparison using Bayes Factors, is in such case the main tool to be used in this context, as far as predictive power is concerned (Hoeting et al., 1999). In particular, this idea should be used when analyzing the numerical vs. the theoretical versions of the resulting posterior distribution. That is, the forward map, defined as the solution of a system of ODE's (or PDE's), represents a complex regressor that is only theoretically defined. The actual usage of the model necessarily involves a numerical solver that includes an approximation error depending on the solver step size h. Therefore, there is a theoretical posterior distribution $P_{\Theta|Y}(\theta|y)$ and the approximate $P^h_{\Theta|Y}(\theta|y)$ posterior. Recently a series of papers (eg. Schwab and Stuart, 2012) discuss regularity conditions under which the latter tends to the former as the approximation error tends to zero, using a suitable metric. A metric comparison (ie. $||P_{\Theta|Y}(\cdot|y) - P^h_{\Theta|Y}(\cdot|y)||$) is useful to proving the required convergence theorems, but more practical considerations will be needed when evaluating the relative benefits of a numerical approach with a particular solver step size h (for data y).

We believe that both $P_{\Theta|Y}(\cdot|y)$ and $P^h_{\Theta|Y}(\cdot|y)$ (and $P^{h_i}_{\Theta|Y}(\cdot|y)$ for any other

h_i) should be compared as *models*, being $P_{\Theta|Y}(\cdot|y)$ the reference but computationally very expensive or even only theoretically available model and the approximate, for various solver precisions $h_1, h_2, \ldots$, as alternative, less computationally demanding computing models. Bayes factors may then be used to establish a sound comparison, to balance predictive power on the one hand vs. solver CPU time on the other, to establish a useful solver precision (that may even be far less precise than common usage but achieve comparable results relative to the observations errors, the model characteristics etc. for the problem at hand). One difficulty here is that in most real applications the theoretical model is unavailable. We therefore establish how to approximate the Bayes factors, without having the theoretical reference model, using solely the numerical solver approximation rates.

1.2 Notation

Assume that we observe a process $\mathbf{y} = (y_1, \ldots, y_n)$ at the discrete times $t_1, \ldots, t_n \in [0, T[^n$ such that

$$y_i = f(X_\theta(t_i)) + \varepsilon_i, \quad \varepsilon_i \sim_{i.i.d.} \mathcal{N}(0, \sigma^2) \qquad (\mathcal{M}) \qquad (1)$$

where X_θ is the solution of the following system of ordinary differential equations, namely the Forward Model,

$$\frac{dX_\theta}{dt} = F(X_\theta, t, \theta); \quad X_\theta(t_0) = X_0. \qquad (2)$$

$\theta \in \Theta \subset \mathbb{R}^d$ is a vector of unknown parameters. $F : \mathbb{R}^p \times [0, T[\times \Theta \mapsto \mathbb{R}^p$ is a known function, whose regularity properties ensure the existence of a unique solution of the initial value problem (2) (the regularity conditions of F will be discussed in Section 2).

$f : \mathbb{R}^p \to \mathbb{R}^k$ in (1) is the observation function. Many types of observation functions f can be considered, modeling for instance the observation of a single component of the p-vector $X_\theta(t)$ or a (linear) combination of the components. In this paper, for the sake of simplicity, we consider a one dimensional observations problem only, that is $k = 1$. Generalizations of our results to multivariate observations are possible and will be briefly mentioned in the Section 6.

Any statistical decision from the data $\mathbf{y}$ –such as estimation, prediction or model selection– relies on the likelihood function (in a Bayesian and other paradigms)

$$P_{\mathbf{Y}|\phi}(\mathbf{y}|\theta, \sigma) = \sigma^{-n} (2\pi)^{-n/2} \exp\left\{ -\frac{1}{2\sigma^2} \sum_{i=1}^n (y_i - f(X_\theta(t_i)))^2 \right\} \qquad (3)$$

whose expression involves the computation of X_θ, a solution of (2). However, except in very simple cases, an explicit expression of the solution is in general not available (although its existence is ensured by regularity assumptions on F).

As a consequence, in practice, the system (2) is solved using a numerical solver and the inference is performed, not on the previous "exact" model but on an approximate model, namely

$$y_i = f(X_\theta^h(t_i)) + \varepsilon_i, \quad \varepsilon_i \sim_{i.i.d.} \mathcal{N}(0, \sigma^2) \qquad (\mathcal{M}_h) \qquad (4)$$

where X_θ^h denotes the approximate solution of (2) supplied by the numerical solver (h being a precision parameter of the solver). The new likelihood derived from model $\mathcal{M}_h$ is thus

$$P_{\mathbf{Y}|\phi}^h(\mathbf{y}|\theta, \sigma) = \sigma^{-n}(2\pi)^{-n/2} \exp\left\{-\frac{1}{2\sigma^2}\sum_{i=1}^{n}(y_i - f(X_\theta^h(t_i)))^2\right\}. \qquad (5)$$

Changing from the original statistical model is obviously not without consequences. Since there is no alternative but to use the approximate model above (4), there exists a real need in understanding and controlling related consequences. In a Bayesian paradigm, any decision is based on the posterior distribution. A first natural choice is to compare the posterior distributions calculated from models ($\mathcal{M}$) and ($\mathcal{M}_h$). Such a study has been proposed by, for example, Donnet and Samson (2007). However, when comparing models in a Bayesian context, the natural tools are Bayes Factors. In this work, we recall their importance, propose an efficient way to compute them in this context and study some theoretical aspects of their calculation when the exact model is not available.

The paper is organized as follows. In Section 2 we discuss the choice of a solver and its required properties from a Bayesian Inverse Problem point of view. Bayesian inference is presented in Section 3 and some control results on the posterior distributions are cited in Subsection 3.2. Bayes factors are introduced and our main theoretical results are developed in Section 4 . Our results are illustrated both with a simulation study and with real data in Section 5. Finally, a discussion of the paper is presented in Section 6.

2 ODE solvers from a Bayesian Inverse problem point of view

Bayesian analysis for inverse problems strongly relies on the numerical approximation of the underlying ODE system. One can choose to use a standard (more or less advanced) implemented solver as a black-box in a sense assuming that no approximation is made on the model. But in our approach, we aim at understanding the influence of this approximation. As a consequence, we are interested in the inherent properties of the numerical solver. When it comes to qualifing a numerical solver, three properties arise, namely its error (local or global), its stability and its stiffness. The three of them are addressed in the following section although global error is surely the most important one as far as the purposes of the paper are concern.

Only a restricted number of nonlinear ODEs has a solution in closed form. Consequently, there is a plethora of numerical methods to solve the initial value problem (2). Noteworthy are time-stepping methods based on Taylor approximation of the function F, multi-step methods and Runge-Kutta methods. These methods span through many orders of local accuracy. Beside the order of accuracy, standard requirements for a numerical method are consistency, convergence, and stability (Iserles, 1996; Quarteroni et al., 2007). However, even when these latter conditions hold, a common concern in the numerical solution of the initial value problem (2) is error control.

Two types of error can be considered, namely the local and the global errors. In the following, we use the theory developed in Quarteroni et al. (2007) to discuss the relationship between local and global errors for one-step Euler and fourth order explicit Runge-Kutta methods.

Let h be the step size of the method. We define a time grid as $t_{n+1} = t_n + h$, for some fixed $h > 0$. Let $X_{\theta,n}$ be the solver approximation of $X_\theta(t_n)$. One-step Euler and fourth order explicit Runge-Kutta methods have the form

$$X_{\theta,n+1} = X_{\theta,n} + hK(t_n, X_{\theta,n}, h, F), \tag{6}$$

where

$$K(t_n, X_{\theta,n}, h, F) = \begin{cases} K_1 & \text{for Euler} \\ \frac{1}{6}(K_1 + 2K_2 + 2K_3 + K_4) & \text{for 4th ord. Runge-Kutta,} \end{cases} \tag{7}$$

with

$$\begin{array}{llll} K_1 & = & F(X_{\theta,n}, t_n, \theta) & K_2 & = & F(X_\theta + \frac{1}{2}hK_1, t_n + \frac{1}{2}h, \theta) \\ K_3 & = & F(X_\theta + \frac{1}{2}hK_2, t_n + \frac{1}{2}h, \theta) & K_4 & = & F(X_\theta + hK_1, t_n + h, \theta). \end{array}$$

(There is also a 2nd order Rungue-Kutta, which will be used in Section 5.1, but we avoid presenting its details.)

Local truncation error e_n is the error made in one step of the numerical method, that is

$$e_n = e_h(t_n, \theta) = ||X_\theta(t_n) - X_\theta(t_{n-1}) - hK(t_n, X_\theta(t_{n-1}), h, F)||_2.$$

Global error E_n is the difference between the computed solution and the true solution at any given value of t belonging to the grid

$$E_n = E_h(t_n, \theta) = ||X_\theta(t_n) - X_{\theta,n}||_2.$$

For (order one) Euler and fourth order Runge-Kutta methods e_n is $O(h^2)$ and $O(h^5)$ respectively (we avoid the details for order two Rungue-Kutta, for which indeed e_n is $O(h^3)$). Proposition 1 establishes a relationship between global and local error for one-step numerical methods like Euler and Runge-Kutta.

Assumption 1. *We assume throughout the paper that the function F in the right hand side of the initial value problem (2) is continuously differentiable with respect to X_θ on a parallelepiped $\mathcal{R} = \{: t_0 \le t \le t_0 + a, \, ||X_\theta - X_0||_2 \le b\}$ for each θ. Hence a unique solution of the initial value problem exists in a neighborhood of (t_0, X_0) for each θ. F as above implies K is Lipschitz continuous on X_θ, i.e. there is $L \in \mathbb{R}^{+*}$ such that if (t, x), $(t, y) \in R$, then*

$$||K(t, x, h, F) - K(t, y, h, F)||_2 \le L||x - y||_2.$$

Proposition 1. *Assume that* Assumption 1 *holds and for the solver at hand and the local truncation error e_n is $O(h^{p+1})$. Then the global truncation error is $O(h^p)$.*

Proof. We have

$$E_n = ||X_\theta(t_n) - X_{\theta,n}||_2 = ||X_\theta(t_n) - X_{\theta,n-1} - hK(t_n, X_{\theta,n-1}, h, F)||_2.$$

Adding and susbtracting the term $X_\theta(t_{n-1}) + hK(t_n, X_\theta(t_{n-1}), h, F)$ we obtain

$$
\begin{aligned}
E_n &\le e_n + ||X_\theta(t_{n-1}) - X_{\theta,n-1}||_2 + h||K(t_n, X_\theta(t_{n-1}), h, F) - K(t_n, X_{\theta,n-1}, h, F)||_2 \\
&\le e_n + E_{n-1} + hL||X_\theta(t_{n-1}) - X_{\theta,n-1}||_2 \\
&\le e_n + E_{n-1}(1 + hL).
\end{aligned}
$$

Consequently

$$
\begin{aligned}
E_n &\le e_n + e_{n-1}(1 + hL) + \ldots + e_1(1 + hL)^{n-1} \\
&\le Hh^{p+1} \frac{1 - (1 + hL)^n}{1 - (1 + hL)} = \frac{H}{L} h^p \{(1 + hL)^n - 1\}.
\end{aligned}
$$

Therefore, since $h = \frac{l}{n}$ $(l = t_n - t_1)$,

$$E_n \le \frac{H}{L} h^p \left\{ \left(1 + \frac{lL}{n}\right)^n - 1 \right\} \le \frac{H}{L} e^{lL} h^p.$$

$\square$

From Proposition 1, we deduce that, for any explicit one-step method of order p such as Euler $(p = 1)$ and Runge-Kutta $(p = 2$ or $p = 4)$ schemes, the global error is of order $O(h^p)$ for h small enough. If we set $X_\theta^h(t_n) = X_{\theta,n}$, note that we have proved that

$$\max_{t \in \{t_1, t_2, \ldots, t_n\}} ||X_\theta(t) - X_\theta^h(t)|| \le C_\theta h^p$$

since H and L above depend on θ. This global error order control will be needed in Sections 3.2 and 4.2 to prove our main result.

In the numerical community, the control of the error means keeping the error e_n or E_n under a fixed level (beyond the above mentioned asimptotic results),

along the application of the scheme. The local error e_n can be controlled directly, using for instance, the "Milne device" (Iserles, 1996). However, there are not known general methods to control global error E_n, although some methods exist to estimate it, for instance, those relying on adjoint state analysis, see Cao and Petzold (2004); Lang and Verwer (2007). In the results that follow we do not require an estimation of this global (or local) error, solely the knowledge of the global error order for the solver at hand.

Another important issue in the numerical solution of problem (2) is stiffness. According to Lambert (1991), if a numerical method with finite region of absolute stability applied to system (2) is forced to use in a certain interval in t a steplength excessively small in relation to the smoothness of the exact solution in that interval, then system (2) is said to be stiff in that interval. We remark that many systems of ODE modeling real life phenomena are stiff, see Gutenkunst et al. (2007).

Software implementing time-stepping methods mentioned above must address error control, stability and stiffness issues. Actually, local error control mechanisms can cope with stiffness at the expense of taking very small stepsizes. Therefore, advanced features like variable order methods, and variable stepsize methods have been developed and implemented in libraries of common high level programing languages like R, Matlab and Python-Scipy.

The results shown in this paper assume a fixed step method. We only work with the Euler and Rugue-Kutta methods (orders $p = 1, 2, 4$ respectively).

3   Bayesian inference for inverse problems: practical and theoretical aspects

There are some excellent reviews concerning the Bayesian analysis of Inverse Problems (Kaipio and Somersalo, 2005; Fox et al., 1999) and for a more detailed description these or other sources should be consulted. In this section we only present the particular aspects of the field relevant to the development of our results.

Any Bayesian statistical decision (such as estimation) is based on the posterior distribution, given by the Bayes formula

$$P^h_{\Phi|\mathbf{Y}}(\theta, \sigma|\mathbf{y}) = \frac{P^h_{\mathbf{Y}|\Phi}(\mathbf{y}|\theta, \sigma)P_\Phi(\theta, \sigma)}{P^h_{\mathbf{Y}}(\mathbf{y})} \tag{8}$$

where $P_\Phi(\theta, \sigma)$ is the prior distribution on (θ, σ) and

$$P^h_{\mathbf{Y}}(\mathbf{y}) = \int P^h_{\mathbf{Y}|\Phi}(\mathbf{y}|\theta, \sigma)P_\Phi(\theta, \sigma)d\theta d\sigma$$

is the normalization constant, also called the *marginal likelihood* of data $\mathbf{y}$.

An estimator of (θ, σ) is derived from some characteristics of the posterior distribution. Various approaches can be adopted. Either the estimator is taken as the mode of the posterior distribution, resulting into the MAP estimator $(\hat{\theta}^{MAP}, \hat{\sigma}^{MAP}) = \arg\max_{(\theta,\sigma)} P^h_{\Phi|\mathbf{Y}}(\theta, \sigma|\mathbf{y})$ or the estimator derives from the minimization of a loss function $L(\theta, \sigma|\eta)$, that is $(\hat{\theta}, \hat{\sigma}) = \arg\min_{(\theta,\sigma)} \int L(\theta, \sigma|\eta) P^h_{\Phi|\mathbf{Y}}(\theta, \sigma|\mathbf{y}) d\theta d\sigma$. If the loss function $L(\theta, \sigma|\eta)$ is equal to the L^2-distance, then the corresponding estimator is the posterior mean $(\hat{\theta}^{L^2}, \hat{\sigma}^{L^2}) = \int (\theta, \sigma) P^h_{\Phi|\mathbf{Y}}(\theta, \sigma|\mathbf{y}) d\theta d\sigma$. If the loss function $L(\theta|\eta)$ is equal to the L^1-distance, then the corresponding estimator is the posterior median, that is $(\hat{\theta}^{L^1}, \hat{\sigma}^{L^1}) = (F^h)^{-1}_{\Phi|\mathbf{Y}}\left(\frac{1}{2}\right)$, etc. In general, posterior expectations of all types (ie. $\int g(\phi) P^h_{\Phi|\mathbf{Y}}(\phi|\mathbf{y}) d\phi$, for some measurable function g) are used to explore the posterior distribution, and these include all marginal distributions for individual parameters or posterior probabilities of specific regions of interest.

Besides some few simple conjugate models, the normalizing constant $P^h_{\mathbf{Y}}(\mathbf{y})$ has no explicit analytic expression and therefore the above estimators can not be directly calculated. If the dimension of Φ is 1 or 2 we could rely on numerical integration to obtain the normalizing constant $P^h_{\mathbf{Y}}(\mathbf{y})$. In larger dimensions, the standard solution is to resort to Monte Carlo methods to approximate the estimators. Let $(\theta^{(l)}, \sigma^{(l)})_{i=1...L}$ be a sample from the posterior distribution, the L^2 estimator for instance, is approximated as $(\hat{\theta}^{L^2}, \hat{\sigma}^{L^2}) = \left(\frac{1}{L}\sum_{l=1}^{M} \theta^{(l)}, \frac{1}{L}\sum_{l=1}^{L} \sigma^{(l)}\right)$.

Simulation from the posterior distribution is not a direct task and Markov Chain Monte Carlo algorithms (see Robert and Casella, 2004, for a didactic review) are standard tools to sample from the posterior distribution $P^h_{\Phi|\mathbf{Y}}(\theta, \sigma|\mathbf{y})$. However, such algorithms have to be carefully designed when the evaluation of the regression function of the model (and consequently of the likelihood function) is computationally intensive. In the next section, we recall the basics of MCMC algorithms and discuss their application to inverse problems and the calculation of Bayes' Factors.

3.1 Sampling from the posterior distribution in Inverse problems

Markov Chain Monte Carlo (MCMC) is specially suited for sampling from complex multidimensional distributions and is ubiquitous in modern Bayesian analyses. We do not intend to present a comprehensive review of MCMC here but merely state the basic principles to consider some aspects of implementing MCMC in the Inverse Problem context; otherwise the reader is referred to Robert and Casella (2004). The principle of MCMC algorithms is to generate a Markov chain whose invariant distribution is the distribution of interest $P^h_{\Phi|\mathbf{Y}}(\theta, \sigma|\mathbf{y})$. Many versions have been proposed in the literature. Among those, the Gibbs algorithm and the Metropolis-Hasting algorithms are the most used and quickly described below.

The Gibbs sampler is a very popular MCMC algorithm. However, only in canonical cases (eg. conditional conjugacy) it make sense to be used. In our Inverse Problem settings, this is not the case and the general Metropolis-Hastings MCMC algorithm needs to be used instead.

The Metropolis-Hastings (MH) algorithm starts by defining a proposal (or instrumental) conditional distribution $q(\phi'|\phi)$, which we are able to simulate from for any ϕ in the support of the posterior distribution. At iteration (ℓ):

1. a proposed value ϕ' is simulated given the current state of the Markov Chain $\phi^{(\ell)}$ from the proposal $q(\cdot|\phi^{(\ell)})$;

2. the proposed point ϕ' is accepted as the new point in the Markov chain $\phi^{(\ell+1)}$ with probability $\rho(\phi^{(\ell)}, \phi')$:

$$phi^{(\ell+1)} = \begin{cases} \phi' & \text{with probability} \quad \rho(\phi^{(\ell)}, \phi') \\ \phi'^{(\ell)} & \text{with probability} \quad 1 - \rho(\phi^{(\ell)}, \phi') \end{cases}$$

where the acceptance probability $\rho(\phi^{(\ell)}, \phi')$ is equal to

$$\begin{aligned} \rho(\phi^{(\ell)}, \phi') &= \min\left\{1, \frac{P^h_{\Phi|\mathbf{Y}}(\phi'|\mathbf{y})}{P^h_{\Phi|\mathbf{Y}}(\phi^{(\ell)}|\mathbf{y})} \frac{q(\phi^{(\ell)}|\phi')}{q(\phi'|\phi^{(\ell)})}\right\} \\ &= \min\left\{1, \frac{P^h_{\mathbf{Y}|\Phi}(\mathbf{y}|\phi')P_\Phi(\phi')}{P^h_{\mathbf{Y}|\Phi}(\mathbf{y}|\phi^{(\ell)})P_\Phi(\phi^{(\ell)})} \frac{q(\phi^{(\ell)}|\phi')}{q(\phi'|\phi^{(\ell)})}\right\}. \end{aligned}$$

Commonly a series of proposal distributions $q_1, q_2, \ldots, q_m$ are entertained, leading to a series of m transition kernels that are systematically or randomly scanned (the latter leads to the desirable reversibility property) to form an easily provable convergent chain to the posterior $P^h_{\Phi|\mathbf{Y}}(\cdot|\mathbf{y})$.

In any case, at each iteration of the MH MCMC we need to evaluate the (unnormalized) posterior (It is therefore crucial to minimize the number of iterations in the MCMC and the number of likelihood evaluations).

Optimizing MCMC algorithms (that is to say minimizing the number of iterations) has been a very active research topic in the last decade. There are adaptive algorithms (Haario et al., 1998; Atchadé and Rosenthal, 2005) that try to learn from previous steps of the chain to adapt the proposals $q_1, \ldots, q_m$. These methods require additional regularity conditions on the adaptive scheme, model and prior that might limit their applicability. Christen and Fox (2010) also propose the t-walk, which self adjusts keeping two points in the parameter space, and that commonly samples with reasonable efficiency. However, robust, multipurpose, automatic and optimal methods are still far away in the MCMC horizon (to make an optimistic metaphor).

When it comes out to inverse problem specifically, various savings can be considered.

• First, a naive but straightforward computational economy is to save $U^{(\ell)} = -\log P^h_{\mathbf{Y}|\Phi}(\mathbf{y}|\phi^{(\ell)}) - \log P_\Phi(\phi^{(\ell)})$. Indeed, this quantity will be used for any new simulated value ϕ' until the chain reaches a new point $\phi^{(\ell+1)}$. We will see in Section 4.1 that these quantities can also be recycled for model comparison purposes. Note that these $U^{(\ell)}$ are very useful for convergence analysis.

• Second, in this Inverse Problem setting we may exploit the possibility that a coarser numerical solver with a higher error rate (or equivalently a larger step size h_1) might lead to a far less CPU demanding approximate calculation of the likelihood $P^{h_1}_{\mathbf{Y}|\phi}(\mathbf{y}|\phi^{(i)})$. More precisely, Christen and Fox (2005) suggest to propose a candidate ϕ' and test its promising acceptance probability using an approximate and cheap calculation of the likelihood (using the coarser numerical solver). If this ϕ' has a "good" probability to being accepted, the full blow and expensive calculation of the likelihood is used to firmly accept or reject ϕ'. This two-step or "delay acceptance MH" algorithm may save substantial CPU time during the MCMC (see Christen and Fox, 2005).

3.2 Theoretical results on the error control of the approximate posterior distribution

After having examined how the standard algorithmic tools for Bayesian inference can be adapted or designed specifically to the Inverse problem context, we may want to understand and control the consequences implied by the use of an approximate model from a theoretical point of view. Such a result can be found in Donnet and Samson (2007) who compare the posterior distributions of the exact and approximate models respectively –namely $P_{\Phi|\mathbf{Y}}$ and $P^h_{\Phi|\mathbf{Y}}$– through the total variation distance.

Proposition 2. *Assume that $\phi = (\theta, \sigma)$ remains in a compact set and that the numerical scheme of step size h is such that $\{t_1, \ldots, t_n\} \subset h\mathbb{N}$ and*

$$\max_{t \in \{t_1, \ldots, t_n\}} \|X_\theta(t) - X^h_\theta(t)\|_{\mathbb{R}^p} \leq C_\theta h^p. \tag{9}$$

Also assume that the observation function f is differentiable with a bounded derivative. Then there exists a constant $C_{\mathbf{y}}$ such that for every (θ, σ) and h small enough

$$|P_{\Phi|\mathbf{Y}}(\theta, \sigma; \mathbf{y}) - P^h_{\Phi|\mathbf{Y}}(\theta, \sigma; \mathbf{y})| \leq C_{\mathbf{y}} \pi(\theta, \sigma) h^p. \tag{10}$$

As a consequence,

$$D_{T.V}(P_{\Phi|\mathbf{Y}}, P^h_{\Phi|\mathbf{Y}}) \leq C_{\mathbf{y}} h^p \tag{11}$$

where $D_{T.V}$ is the total variation distance. Moreover,

$$\|(\hat{\theta}^{L^2}, \hat{\sigma}^{L^2}) - (\hat{\theta}^{h,L^2}, \hat{\sigma}^{h,L^2})\| \leq h^p C'_{\mathbf{y}} \tag{12}$$

Proof. Donnet and Samson (2007)'s results are developed for mixed effects models in a maximum likelihood context but can be adapted to models (1) and (4). Inequality (10) is derived from Theorem 4 of Donnet and Samson (2007). The control on the total variation distance is derived directly. The inequality (12) is obtained as follows

$$
\begin{aligned}
&\|(\hat{\theta}^{L^2}, \hat{\sigma}^{L^2}) - (\hat{\theta}^{h,L^2}, \hat{\sigma}^{h,L^2})\| \\
&= \| \int (\theta,\sigma) P_{\Phi|\mathbf{Y}}(\theta,\sigma|\mathbf{y})d\theta - \int (\theta,\sigma) P_{\Phi|\mathbf{Y}}^h(\theta,\sigma|\mathbf{y})d\theta d\sigma\| \\
&= \| \int (\theta,\sigma) \left[P_{\Phi|\mathbf{Y}}(\theta,\sigma|\mathbf{y}) - P_{\Phi|\mathbf{Y}}^h(\theta,\sigma|\mathbf{y}) \right] d\theta d\sigma\| \\
&\leq \int \|(\theta;\sigma)\| C_\mathbf{y} P_\Phi(\theta,\sigma) h^p d\theta d\sigma \\
&\leq h^p C_\mathbf{y} \int \|(\theta;\sigma)\| P_\Phi(\theta,\sigma) d\theta d\sigma
\end{aligned}
$$

$\square$

Note that obtaining the same type of control on the MAP estimator requires additional regularity assumptions on the posterior distributions, such as unicity of the extremum and properties on the second derivatives. This leads to encourage the use of L^2 estimates over the MAP estimates in this context.

Cotter et al. (2010) also proposes control results of the same type. Even if these results provide interesting theoretical error controls, they rely on unknown constants and so can not be used as such in practice. In the next section, we adopt a Bayes factor point of view and highlight that such an approach leads to results of more practical interest.

4 Model selection and Bayes Factor for inverse problems

In Bayesian inference, model selection is performed using the Bayes factors whose principle is recalled here in a general context. Let $\mathbf{y}$ be the observations and let $\mathcal{M}_1$ and $\mathcal{M}_2$ be two models in competition. Each model $\mathcal{M}_i$ is defined through a likelihood depending on a set of parameters and a prior distribution on the parameters. More precisely,

$$
(\mathcal{M}_1) \begin{cases} \mathbf{y} & \sim & P_{\mathbf{Y}|\Phi_1}^1(\mathbf{y}|\phi_1) \\ \phi_1 & \sim & P_{\Phi_1}^1(\phi_1) \end{cases} \qquad (\mathcal{M}_2) \begin{cases} \mathbf{y} & \sim & P_{\mathbf{Y}|\Phi_2}^2(\mathbf{y}|\phi_2) \\ \phi_2 & \sim & P_{\Phi_2}^2(\phi_2) \end{cases} .
$$

Consider a prior distribution on the set of the models $\{\mathcal{M}_1, \mathcal{M}_2\}$, the decision between the competing models $\mathcal{M}_1$ and $\mathcal{M}_2$ is based on the ratio of their respective posterior probabilities

$$
\frac{P(\mathcal{M}_2|\mathbf{y})}{P(\mathcal{M}_1|\mathbf{y})} = \frac{P_\mathbf{Y}^2(\mathbf{y})}{P_\mathbf{Y}^1(\mathbf{y})} \frac{P(\mathcal{M}_2)}{P(\mathcal{M}_1)}
$$

where $P_\mathbf{Y}^i(\mathbf{y})$ is the 'integrated likelihood' or the marginal distribution of $\mathbf{Y}$ of model $\mathcal{M}_i$, namely

$$
P_\mathbf{Y}^i(\mathbf{y}) = \int P_{\mathbf{Y}|\Phi_i}^i(\mathbf{y}|\phi_i) P_{\Phi_i}(\phi_i) d\phi_i.
$$

Finally, the comparison of models relies on the computation of the marginal likelihoods which has been the object of a rich literature. Two approaches may be cited. One consist in running a specific MCMC to approximate the quantity of interest (see Han and Carlin, 2001, for a review). The second relies on Monte Carlo approximations of the marginal likelihood $P_{\mathbf{Y}}^i(\mathbf{y})$ (see for instance Chen and Shao, 1997).

4.1 Computation of Bayes Factors in an Inverse Problem context

In our inverse problem context –where each iteration of the MCMC requires the computationally intensive approximation of an ODE – we would like to avoid increasing the computational burden by using a specific MCMC and would prefer recycling the outputs of the MCMC algorithm into a Monte Carlo strategy. An answer can be found in the Gelfand and Dey's estimator (Gelfand and Dey, 1994).

More precisely, a standard solution to compute the marginal likelihood is to propose an estimation based on a Monte Carlo approximation. Let $\{\phi_i^{(l)}\}_{l=1\ldots L}$ be an i.i.d. sample from a proposal distribution π_{IS} then the following estimator

$$\widehat{p}_i = \frac{1}{L} \sum_{l=1}^{L} P_{\mathbf{Y}|\Phi_i^{(l)}}^i(\mathbf{y}|\phi_i^{(l)}) \frac{P_{\Phi_i}(\phi_i^{(l)})}{\pi_{IS}(\phi_i^{(l)})}$$

supplies a convergent and non biased estimator of $P_{\mathbf{Y}}^i(\mathbf{y})$. However, in the inverse problems context (when one or both models $\mathcal{M}_i$ are defined through ODE without explicit solution) such a strategy requires the evaluation of the likelihood and thus the evaluation of an approximate solution of the dynamical system for each newly generated value of parameters $\phi_i^{(l)}$, which can be burdensome from a computational time point of view.

The Gelfand and Dey's estimator is an alternative solution to this situation. Assume that (as it is in standard situations), $P_{\Phi|\mathbf{Y}}^h(\theta, \sigma|\mathbf{y})$ is sampled using an intensive Monte Carlo procedure, typically a Metropolis-Hasting MCMC. (Note that for ease of presentation we avoid the exponent i or h and, notationally, consider the posterior distribution $P_{\Phi|\mathbf{Y}}(\theta, \sigma|\mathbf{y})$ and estimation of the normalization constant $P_{\mathbf{Y}}(\mathbf{y})$)

Assume that the prior distribution P_Φ is absolutely continuos w.r.t the Lebesgue measure, and thus $P_\Phi(\theta, \sigma)$ and $P_{\Phi|\mathbf{Y}}(\theta, \sigma|\mathbf{y})$ are densities in the usual sense. The Gelfand and Dey's estimator relies on the obvious following expression

$$[P_{\mathbf{Y}}(\mathbf{y})]^{-1} = \int \frac{\alpha(\theta, \sigma)}{P_{\mathbf{Y}|\Phi}(\mathbf{y}|\theta, \sigma) P_\Phi(\theta, \sigma)} P_{\Phi|\mathbf{Y}}(\theta, \sigma|\mathbf{y}) d\theta d\sigma,$$

where α is any density ($\int \alpha(\theta, \sigma) d\theta d\sigma = 1$) with support containing the support of the posterior.

12

Now, let $\theta^{(1)}, \sigma^{(1)}, \theta^{(2)}, \sigma^{(2)}, \ldots, \theta^{(L)}, \sigma^{(L)}$ be a MCMC sample of the posterior $P_{\Phi|\mathbf{Y}}(\theta, \sigma | \mathbf{y})$. Considering the above expression, the desired marginal may be approximated by

$$\widehat{P}_{\mathbf{Y}}(\mathbf{y}) = \left[\frac{1}{L} \sum_{l=1}^{L} \frac{\alpha(\theta^{(l)}, \sigma^{(l)})}{P_{\mathbf{Y}|\Phi}(\mathbf{y}|\theta^{(l)}, \sigma^{(l)}) P_{\Phi}(\theta^{(l)}, \sigma^{(l)})} \right]^{-1}. \tag{13}$$

The choice of α conditions the quality of the estimator (its variance). If $\alpha(\theta, \sigma) = \pi(\theta, \sigma)$, the estimator $\widehat{P}_{\mathbf{Y}}(\mathbf{y})$ is the harmonic mean which is known to have a dramatic unstable behaviour (infinite variance) in some cases. Best strategies are those that use a weighting α density that stabilizes this estimators, for instance using somehow an α that resembles $P_{\mathbf{Y}|\Phi}(\mathbf{y}|\theta, \sigma) P_{\Phi}(\theta, \sigma)$. A simple calculation leads to the fact that using a *thinner* tailed α (as oppose to the result in importance sampling) is better suited to obtaining a finite variance for the estimator above.

Moreover, in an inverse problem context, it is critical to avoid recalculating the likelihood $P_{\mathbf{Y}|\Phi}(\mathbf{y}|\theta, \sigma)$ since it involves numerically solving the ODE system in (2). As a consequence we propose to proceed as follows.

• At each iteration of a typical MH MCMC, the computation of the probability of acceptation requires to evaluate $P_{\Phi|\mathbf{Y}}(\mathbf{y}|\theta^{(l)}, \sigma^{(l)}) P_{\Phi}(\theta^{(l)}, \sigma^{(l)})$. After the burn in period, we save these values, letting $U_l = -\log P_{\Phi|\mathbf{Y}}(\mathbf{y}|\theta^{(l)}, \sigma^{(l)}) - \log P_{\Phi}(\theta^{(l)}, \sigma^{(l)})$.

• A small subsample of $\theta^{(l)}, \sigma^{(l)}$, typically of size less than 1,000, is then used to create a Kernel Density Estimate (KDE), which we will use as our weighting density α. This KDE is (typically) a mixture of Gaussians, with support in the whole space, and will roughly resemble the posterior $P_{\Phi|\mathbf{Y}}$.

• Let $A_i = -\log \alpha(\theta^{(l)}, \sigma^{(l)})$, then our estimate becomes

$$P_{\mathbf{Y}}(\mathbf{y}) \approx \left[\frac{1}{L} \sum_{l=1}^{L} \exp(U_l - A_l) \right]^{-1}.$$

This procedure is fast and basically is a byproduct of the MCMC sample, with little CPU burden added. There are robust and fast KDE's routines available in popular programming languages like R and Python-Scipy.

Remark 1. *Note that $P_{\mathbf{Y}|\Phi}(\mathbf{y}|\theta, \sigma) P_{\Phi}(\theta, \sigma)$ needs to be known exactly, and be coded accordingly which is not the case in some situations, for example, when the prior is not normalized and only implicitly defined etc.*

4.2 Comparing the exact and approximate models through Bayes factors

In section 3.2, we compared the true and approximate models (models 1 and 4) through a derived quantity, that is to say their corresponding posterior distribution or the estimators they supplied. However, a more natural way to compare

models is to use the Bayes factors. Let $(\mathcal{M})$ and $(\mathcal{M}_h)$ be the two following models

$$(\mathcal{M})\begin{cases} y_i & = & f(X_\theta(t_i)) + \varepsilon_i \\ \varepsilon_i & \sim & i.i.d.\mathcal{N}(0,\sigma^2) \\ (\theta,\sigma) & \sim & P_\Phi(\theta,\sigma) \end{cases} \qquad (\mathcal{M}_h)\begin{cases} y_i & = & f(X_\theta^h(t_i)) + \varepsilon_i \\ \varepsilon_i & \sim & i.i.d.\mathcal{N}(0,\sigma^2) \\ (\theta,\sigma) & \sim & P_\Phi(\theta,\sigma). \end{cases}$$

Comparing $\mathcal{M}$ and $\mathcal{M}_h$ through a Bayes factor requires to compute the following quantity

$$B_{\mathcal{M},\mathcal{M}_h} = \frac{P(\mathcal{M}|\mathbf{y})}{P(\mathcal{M}_h|\mathbf{y})} = \frac{\int P_{\mathbf{Y}|\Phi}(\mathbf{y}|\theta,\sigma)P_\Phi(\theta,\sigma)d\theta d\sigma}{\int P_{\mathbf{Y}|\Phi}^h(\mathbf{y}|\theta,\sigma)P_\Phi(\theta,\sigma)d\theta d\sigma}\frac{P(\mathcal{M})}{P(\mathcal{M}_h)}.$$

However, $\int P_{\mathbf{Y}|\Phi}(\mathbf{y}|\theta,\sigma)P_\Phi(\theta,\sigma)d\theta d\sigma$ is not known in general, since it involves the theoretical model. In order to understand the behavior of the Bayes Factor, we study $B_{\mathcal{M},\mathcal{M}_h}$ for small h and obtain the following result.

Proposition 3. *Assume that the numerical solver is such that the global error truncation can be written as*

$$E_h(t,\theta) = X_\theta^h(t) - X_\theta(t) = O(h^p),$$

where h is the stepsize of the method. In addition, assume that the observation function f is differentiable on $\{X_\theta(t), \theta \in \Theta, t \in [0,T]\}$. Then, there exists a constant $B(\mathbf{y}) \in \mathbb{R}$ (which does not depend on h) such that

$$\frac{P_\mathbf{Y}(\mathbf{y})}{P_\mathbf{Y}^h(\mathbf{y})} \simeq 1 + B(\mathbf{y})h^p.$$

Proof. Using the asymptotic behavior of the global error truncation and assuming that f is differentiable, we can write

$$D_h(t,\theta) = f(X_\theta^h(t)) - f(X_\theta(t)) = \nabla f\left(X_\theta(t)\right)\left(X_\theta^h(t) - X_\theta(t)\right) + O(h^p) \quad (14)$$

This approximation allows us to obtain a development of the marginal likelihood. Let $R_h(\phi) = \frac{P_{\mathbf{Y}|\Phi}^h(\mathbf{y}|\theta,\sigma)}{P_{\mathbf{Y}|\Phi}(\mathbf{y}|\theta,\sigma)}$, then

$$\begin{aligned} P_\mathbf{Y}^h(\mathbf{y}) & = & \int P_{\mathbf{Y}|\Phi}^h(\mathbf{y}|\phi)P_\Phi(\phi)d\phi = \int P_{\mathbf{Y}|\Phi}(\mathbf{y}|\phi)R_h(\phi)P_\Phi(\phi)d\phi \\ & = & P_\mathbf{Y}(\mathbf{y}) + \int P_{\mathbf{Y}|\Phi}(\mathbf{y}|\phi)(R_h(\phi)-1)P_\Phi(\phi)d\phi. \end{aligned}$$

We see that

$$\begin{aligned} R_h(\phi) - 1 & = & \exp\left\{-\frac{1}{2\sigma^2}\sum_{i=1}^n \left[f(X_\theta^h(t_i)) - f(X_\theta(t_i))\right]^2 + \right. \\ & & \left. 2\left[y_i - f(X_\theta(t_i))\right]\left[f(X_\theta(t_i)) - f(X_\theta^h(t_i))\right]\right\} - 1 \\ & = & -\frac{1}{2\sigma^2}\sum_{i=1}^n D_h(t_i,\theta)^2 + 2(y_i - f(X_\theta(t_i)))D_h(t_i,\theta) \\ & & +O(D_h(t_i,\theta)^2), \end{aligned} \qquad (15)$$

14

since $e^x - 1 = x + O(x^2)$ for x small enough. Using the expression in (14) for D_h and the solver global error control assumption in (9) we must have that $R_h(\phi) - 1 = O(h^p)$. From this we get

$$P_{\mathbf{Y}}^h(\mathbf{y}) = P_{\mathbf{Y}}(\mathbf{y}) + O(h^p)$$

implying that for h small enough,

$$\frac{P_{\mathbf{Y}}(\mathbf{y})}{P_{\mathbf{Y}}^h(\mathbf{y})} \simeq 1 + B(\mathbf{y})h^p.$$

$\square$

***Corollary* 1.** *If $\hat{g} = \int g(\phi)P_{\Phi|\mathbf{Y}}(\phi|\mathbf{y})d\phi$ and $\hat{g}^h = \int g(\phi)P_{\Phi|\mathbf{Y}}^h(\phi|\mathbf{y})d\phi$ exists, then $|\hat{g}^h - \hat{g}| = \frac{P_{\mathbf{Y}}(\mathbf{y})}{P_{\mathbf{Y}}^h(\mathbf{y})}B_g(\mathbf{y})h^p = O(h^p)$.*

Proof. Note that $|\hat{g}^h - \hat{g}| = \left| \int g(\phi)R_h(\phi)\frac{P_{\mathbf{Y}}(\mathbf{y})}{P_{\mathbf{Y}}^h(\mathbf{y})}P_{\Phi|\mathbf{Y}}(\phi|\mathbf{y})d\phi - \hat{g} \right|$ and therefore $|\hat{g}^h - \hat{g}| = \frac{P_{\mathbf{Y}}(\mathbf{y})}{P_{\mathbf{Y}}^h(\mathbf{y})} \left| \int g(\phi)(R_h(\phi) - 1)P_{\Phi|\mathbf{Y}}(\phi|\mathbf{y})d\phi - \left(\frac{P_{\mathbf{Y}}^h(\mathbf{y})}{P_{\mathbf{Y}}(\mathbf{y})} - 1 \right) \hat{g} \right|$. Combining (15) and the above theorem one reaches the result. $\square$

Regarding the above result, we make the following comments and remarks.

• From (15), we note that the error in the regression term $D_h(t, \theta)$ is not important per se but with respect to the observation noise standard error σ. This obvious remark has consequences. It means that, when working on a statistical model involving the numerical approximation of a differential system, there is no need in choosing a step size the smaller as possible but adapting it such that the global error is small with respect to σ. This can allow computational time savings as illustrated on the following numerical examples.

• Note that $B(\mathbf{y})$ only depends on the numerical method and on the data, but not on the step size h.

• The constant $B(\mathbf{y})$ can be estimated. Indeed, an obvious method is to compute $P_{\mathbf{Y}}^{h_k}(\mathbf{y})$ for various values of step size $\{h_k, k = 1 \ldots K\}$. A simple linear regression of $P_{\mathbf{Y}}^{h_k}(\mathbf{y})$ against h_k^p gives an estimation of $B(\mathbf{y})$. This means that using a multi-resolution computation of the $P_{\mathbf{Y}}^{h_k}(\mathbf{y})$ on various approximate models, we are able to estimate the marginal likelihood of the true model.

• This last point is of major importance. Assume that, two models $\mathcal{M}_1$ and $\mathcal{M}_2$ have to be compared, one or both of them being defined by a differential system without explicit solution. These two models can be compared per se. Indeed, whereas one could have thought that only the approximate models $\mathcal{M}_1^h$ and $\mathcal{M}_2^h$ where comparable, we establish that the both true or exact models $\mathcal{M}_1$ and $\mathcal{M}_2$ may be directly compared.

In the next section, we develop two examples where we estimate the Bayes factor of the theoretically exact model with approximate models. As a consequence the step size may be coarsened, obtaining basically the same posterior distributions, but at far lower CPU costs.
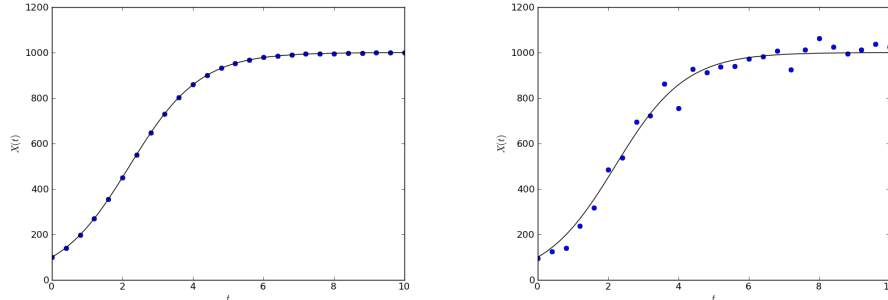
Figure 1: Synthetic data for the Logistic growth with $\lambda = 1$, $K = 1000$ and $\sigma = 1$ (left) or $\sigma = 30$ (right).

5 Numerical examples

5.1 Logistic Growth Models

We base our first numerical study on the logistic growth model which is a common model of population growth in ecology. Recently it has also been used to model tumors growth in medicine, among many other applications. Let $X(t)$ be the size of the tumor to time t. The dynamics are governed by the following differential equation

$$\frac{dX}{dt} = \lambda X(t)(K - X(t)), \quad X(0) = X_0 \tag{16}$$

with $r = \lambda K$ being the growth rate and K the carrying capacity e.g. $\lim_{t \to \infty} X(t) = K$. Equation (16) has an explicit solution equal to

$$X(t) = \frac{K X_0 e^{\lambda K t}}{K + X_0(e^{\lambda K t} - 1)}.$$

We simulate two synthetic data sets with the error model $y_i = X(t_i) + \varepsilon_i$, where $\varepsilon_i \sim \mathcal{N}(0, \sigma^2)$, and the following parameters $X(0) = 100$, $\lambda = 1$, $K = 1000$, $\sigma = 1$ or 30. The datasets are plotted on Figure 1 for the two chosen values of σ. We consider 26 observations at times t_i regularly spaced between 0 and 10.

For this first toy example, K is taken as known and inference is concentrated on the single parameter λ; we consider a Gamma distribution for the prior on λ.

To highlight our result presented in Section 3, we consider the following strategy. For $\sigma = 1$, we first compute what we call the "true" marginal likelihood $P_{\mathbf{Y}}(\mathbf{y})$ (red line in Figure 2), using the explicit solution of (16) and numerical integration. In a second step, we approximate the solution of (16) by the Euler scheme (equivalent to the Runge-Kutta solver of order 1), for various step

16

sizes h_k. The marginal likelihood $P_{\mathbf{Y}}^{h_k(1)}(\mathbf{y})$ is computed using both numerical integration and the Monte Carlo strategy presented in Section 4.1. These results are plotted in black in Figure 2, with solid thin lines for the numerical integration and triangles for the Monte Carlo computation. In a third step, the same strategy is applied but using a Runge-Kutta solver of order 2 (in green in Figure 2). Finally, we use a classical Runge-Kutta solver of order 4 (in green in Figure 2). In the end, for each order p, the estimated values $\hat{P}_{\mathbf{Y}}^{h_k(p)}(\mathbf{y})$ are used to compute the regression functions $\hat{P}_{\mathbf{Y}}^{h_k(p)}(\mathbf{y}) = a + bh^p$ (thick lines in black, green and blue on Figure 2). These results are presented in Figures 2 and 3.

The same is done for $\sigma = 30$ but only the RK solver of order 4 is considered. The equivalent results are presented in Figure 4. The samples from the posterior distributions are obtained using a t-walk MCMC algorithm (Christen and Fox, 2010). Next we discuss some aspects of this numerical experiment.

• We would like to highlight that the thick lines and the triangles are quite similar, meaning that the Monte Carlo strategy (derived as a by-product of the MCMC implementation) is an efficient solution to estimating the marginal likelihood in this context. This approximation has the great advantage of not to involving any new ODE solver runs and thus has a minimal computational cost.

• As predicted, the Euler scheme has a linear approximation regime to the correct marginal. To have any substantial save in CPU without compromising posterior inference precision we would need to have a very small step size, i.e. there is no 'flat part' in order to take considerable larger step sizes. On the contrary, the Runge-Kutta solvers of order 2 and specially the classical RK of order 4, they indeed have a clear flat section where a nearly perfect estimation has been reached. This allows for choosing a much larger step size, meaning a far coarser ODE numerical solver which still has basically no difference in the resulting inference and may be seen in the resulting posterior distributions in Figures 3(b) and 4(c).

• For the RK or order 4, we perform a linear regression using the estimated $\hat{P}_{\mathbf{Y}}^{h_k}(\mathbf{y})$ with $h_k = 0.2$, 0.1, 0.05, 0.025 for $\sigma = 1$ and $h_k = 0.8$, 0.6, 0.4, 0.2, 0.1, 0.05 for $\sigma = 30$. Using the formula given in Proposition 1, we deduce an estimation (projection) of the exact marginal likelihood $\hat{P}_{\mathbf{Y}}(\mathbf{y})$, which has to be compared to the true value $P_{\mathbf{Y}}(\mathbf{y})$ (obtained using the exact solution of the ODE and a numerical integration). The results are given in the following Table 1.

• We believe that the most important message is that, for the RK of order 4, as soon as h is lower than some threshold (we took 0.05 for $\sigma = 1$ and 0.1 for $\sigma = 30$), the Bayes factor ratio $P_{\mathbf{Y}}^{h_k(2)}(\mathbf{y})/P_{\mathbf{Y}}(\mathbf{y})$ is greater than 0.99, making the models indistinguishable on the Jeffrey's Bayesian scale and leading to nearly identical posterior distributions (see Figures 3(b) and 4(c)) for λ. However, the computational time required to estimate the parameters using the smallest h explodes (see Figures 3(a) and 4(b)) from 2 min for $h = 0.05$ to 17 min for
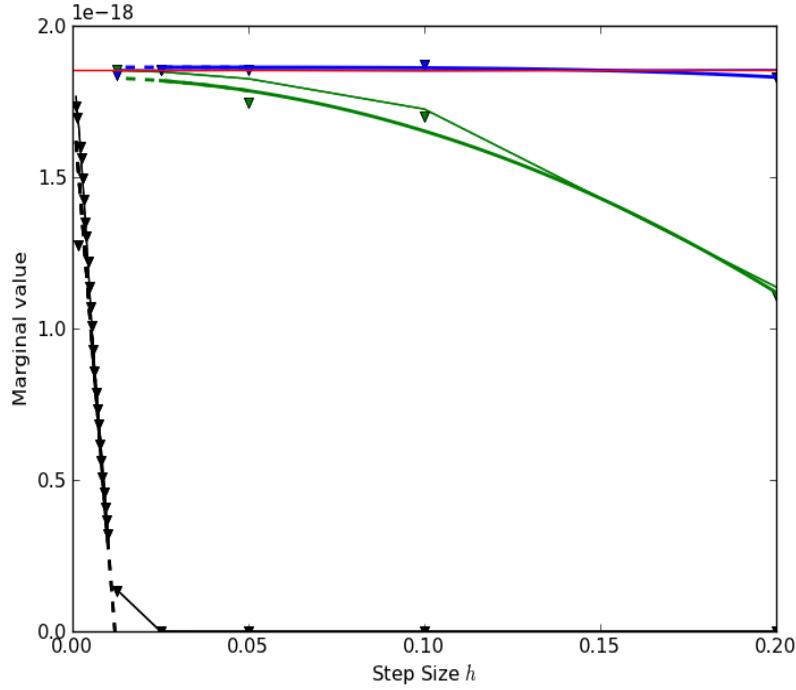
Figure 2: *Study on synthetic data for the Logistic growth with $\sigma = 1$. Marginal $P_{\mathbf{Y}}^h(\mathbf{y})$ for various step sizes, computed by numerical integration (solid thin lines) or estimated using the MCMC sample (triangles). In black, Runge-Kutta solver (RK) of order 1 (Euler), in green RK of order $p = 2$, in blue RK of order $p = 4$. Red line: true marginal $P_{\mathbf{Y}}(\mathbf{y})$ calculated using numerical integration on the analytic solution. Thick lines indicate the regression for estimated values for $\hat{P}_{\mathbf{Y}}^h(\mathbf{y}) = a + bh^p$ for the orders $p = 1, 2, 4$.*

σ	$P_{\mathbf{Y}}(\mathbf{y})$	$\hat{P}_{\mathbf{Y}}(\mathbf{y})$
1	$1.854 \, 10^{-18}$	$1.862 \, 10^{-18}$
30	$1.638 \, 10^{-60}$	$1.699 \, 10^{-60}$

Table 1: Comparison of exact an estimated marginals for the Ringue-Kutta method of order 4.

(a)　　　　　　　　　　　(b)
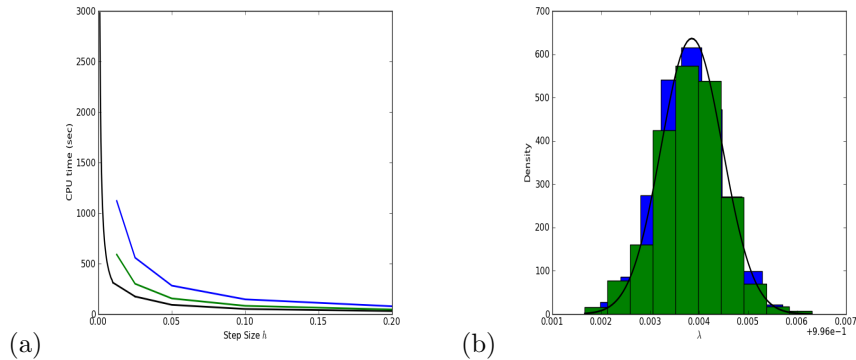
Figure 3: (a) CPU time for various step values h_k and $p = 1, 2, 4$, relative to 10,000 iterations of the MCMC. (b) Posterior distribution of λ the for RK4 solver, $p = 4$, for step sizes $h = 0.01$ and $h = 0.06$ (histograms) and exact posterior (black density). 10,000 iterations of the MCMC took 17 min for $h = 0.01$ and 2 min for $h = 0.05$; a 90% reduction in CPU time with no noticeable difference in the resulting posterior distribution.

$h = 0.01$, for $\sigma = 1$, and from 2.5 min for $h = 0.1$ to 36 min for $h = 0.000625$, for $\sigma = 30$.

• Note that the ranges of considered values for h_k are different for $\sigma = 1$ and $\sigma = 30$. This has to be linked to the remark we have made above: the error induced by the numerical integration of the ODE can not be considered per-se but with respect to the observation noise. When $\sigma = 30$, the step size h^* such that for any $h \leq h^*$ all the models $\mathcal{M}^h$ are equivalent on the Jeffrey's scale is much more higher involving even larger computational time savings.

5.2 A Diabetes minimal model

We know illustrate our results on a real dataset and a more complex model for an Oral Oral Glucose Tolerance Test (OGTT). After having briefly described the experiment and the model, we present our results.

An Oral Glucose Tolerance Test (OGTT) is performed for diagnosis of diabetes, methabolic syndrome and other conditions. After a night sleep, fasting patients are measured for blood glucose and asked to drink a sugar concentrate. Blood glucose is then measured at the hour, two hours and sometime at three hours, depending on local practices. We are developing a minimal model for blood glucose-insulin interaction base on a two compartment model. One simple transfer compartment of glucose in the digestive system and one more complex compartment for blood glucose and interactions with Insulin and other glucose substitution mechanisms. Here we present this model to show

19
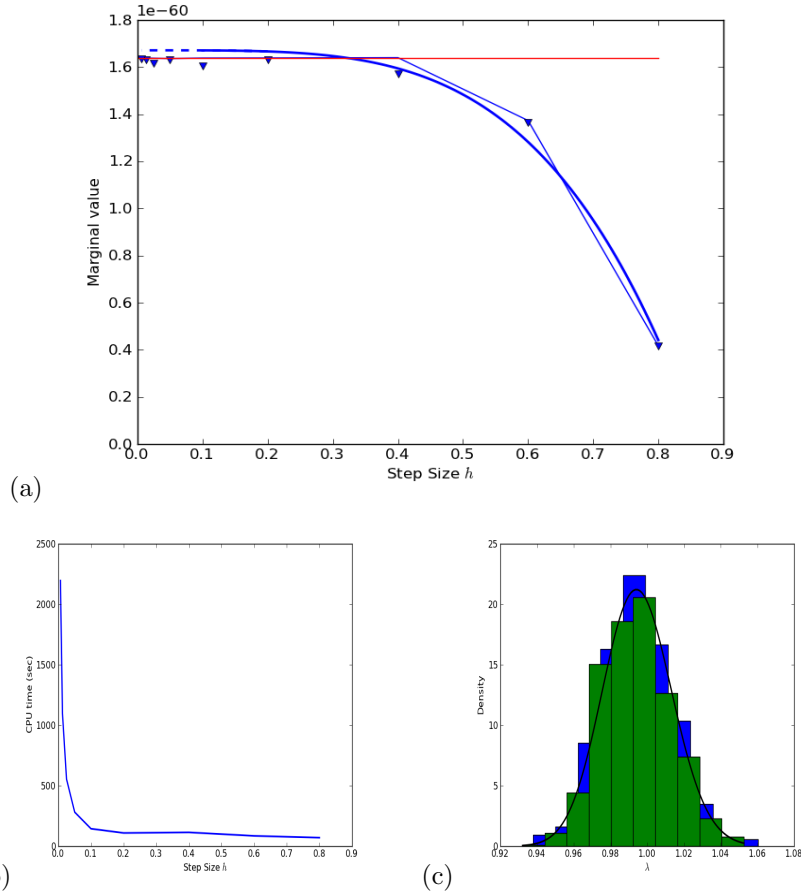
Figure 4: *Study on synthetic data for the Logistic growth with $\sigma = 30$.* (a) Marginal $P_{\mathbf{Y}}^h(\mathbf{y})$ for various step sizes, both exact (solid thin lines, using numerical integration) and estimated using the MCMC sample (triangles). We use a Rungue-Kutta solver of order 4 (classical RK4, blue), only. Red line: true marginal $P_{\mathbf{Y}}(\mathbf{y})$ calculated using numerical integration on the analytic solution. Thick lines indicate the regression for estimated values for $\hat{P}_{\mathbf{Y}}^h(\mathbf{y}) = a + bh^p$ for the order $p = 4$. (b) Corresponding CPU time, relative to 10,000 iterations of the MCMC. (c) Posterior distribution of λ the for RK4 solver, $p = 4$, for step sizes $h = 0.00625$ and $h = 0.1$ (histograms; and exact posterior, black density). The former takes 36 min and the latter 2.5 min.

20

our methodology estimating one parameter only (namely, the insulin sensitivity). Although there is no analytical solution we are able to find the marginal $P_{\mathbf{Y}}^h(\mathbf{Y})$ by numerical integration (since there is only one parameter involved) for comparison purposes.

Let $G(t)$ be blood glucose level at time t, in mg/dL. Let $I(t)$ be blood insulin level at time t and $L(t)$ "glucagon" levels, to promote liver Glycogen glucose production, in arbitrary units. Let $D(t)$ be the digestive system 'glucose level'; we take it as a compartment in which glucose is first stored (eg. stomach and digestive tract) and in turn delivered into the blood stream (we state $D(t)$ in the same units as for $G(t)$ and therefore the mean life parameter θ_2 in (20) is the same as the one used in (17) below). Let also G_b be the glucose base line, (=80 mg/dL, fixed). Our model is described by the following system of differential equations

$$\frac{dG}{dt} = (L - I)\,G + \frac{D}{\theta_2}, \tag{17}$$

$$\frac{dI}{dt} = \theta_0 \left(\frac{G}{G_b} - 1\right)^+ - \frac{I}{a}, \tag{18}$$

$$\frac{dL}{dt} = \theta_1 \left(1 - \frac{G}{G_b}\right)^+ - \frac{L}{b}, \tag{19}$$

$$\frac{dD}{dt} = -\frac{D}{\theta_2}. \tag{20}$$

A brief explanation of the model goes as follows. When glucose goes above the normal threshold G_b, Insulin is produced, ie. its derivative increases, see (18). This, in turn, acts on blood glucose to decrease its concentration; a mass-action type term is introduced in (17) to decrease the derivative of G. L is an abstract term related to the glucose recovery system. When Glucose $G(t)$ goes below the normal threshold (G_b) L increases, see (19), to increase the derivative of $G(t)$ (thus eventually increasing the glucose), see (17). Finally, $D(t)$ represents the glucose in the digestive compartment that will be transferred to the blood stream, see (20) and (17). We analyze data from an OGTT conducted in an obese male adult patient with a suspected methabolic syndrome condition; the corresponding data are plotted on Figure 5. All parameters are positive and will be set to $\theta_1 = 26.6, \theta_2 = 0.2, a = 1, b = 2$, while θ_0 is taken as unknown and will be estimated from data. This is an unusual experimental data set in which Glucose was measured every 30 min up to 2 hr.

Our Bayesian inference is performed as follows. We have observations $d_1, d_2, \ldots, d_n$ for Glucose, thus we let

$$d_i = G(t_i) + e_i \quad \text{where} \quad e_i \sim N(0, \sigma),$$

and $G(0) = d_0$ the initial condition; we fix the measurement error to $\sigma = 5$ (the observation functional is therefore $f(X) = X_1$). From this a likelihood is

21
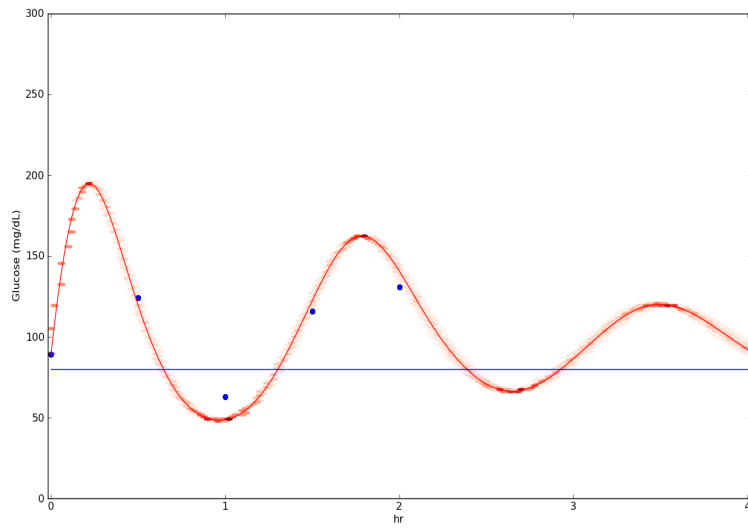
Figure 5: OGTT test performed in an obese male adult, with glucose measurents taken every 30 min up to 2 hr. Note the oscilating nature of the data, typically of a not well control Insulin-Glucose system. Both θ_0 and θ_1 have large values in comparison to normal subjects. The MAP model is shown in red, along with draws from the posterior predictive distribution shown in the shaded areas.

constructed. A Gamma prior distribution is assumed for parameter θ_0, with shape parameter $= 5$ and rate $= 2/5$, thus with mean $= 2$, apparently a value for a normal person. Using an order 4 Rugue-Kutta solver with varying step size we perform a MCMC for these parameters using the t-walk (Christen and Fox, 2010).

To make the solver evaluation time steps (in hr) include the observation times we take a rough time step of 15min ($=0.25$hr) and divide it into finer time steps defined as $h^{(k)} = 0.25 \cdot 2^{-k}$. Our experiments included $k = 0, \ldots, 7$, as seen in in Figure 6(a). We only use an order 4 Runge-Kutta solver, resulting in the 4th grade polynomial regression and a flat section already at $h^{(3)} = 0.25 \cdot 2^{-3} = 1.875$min. If compared with our minimum time step of $h^{(7)} = 0.25 \cdot 2^{-7} = 7$sec, the resulting CPU time of the MCMC is more than 90% larger. However, the resulting posterior distributions for $h^{(3)}$ and $h^{(7)}$ are basically identical (see Figure 6(c)). The estimated marginal is $P_{\mathbf{Y}}^{h^{(3)}}(\mathbf{y}) \approx 3 \cdot 10^{-14}$, calculated using the MCMC samples and (13), while $P_{\mathbf{Y}}^{h^{(7)}}(\mathbf{y}) \approx 3.2 \cdot 10^{-14}$ calculated using numerical integration (red line in Figure 6(a)).

6   Discussion

We advance on some theoretical aspects of the Bayesian analysis of ODE systems. As opposed to more standard (Bayesian) statistical analyses, Inverse Problems present the added difficulty that the regressor function is not analytically tractable and numerical approximations need to be used. In general, the replacement of the theoretical (non-available) solution of the differential system by a numerical approximation is ignored and the solver being used as a black box. However, recently, research has been directed at trying to quantify the consequences of such an approximation, commonly by comparing expected values of the resulting posterior distributions, like the exact vs the numerical Posterior means.

In this paper we adopt a different approach, basing our comparison on the use of Bayes Factors, which is the natural tool to comparing models in a Bayesian context. There are still some particular issues to be solve when applying our results to more realistic inverse problems like estimating the marginals in a multidimensional parameter problem and analyzing stiff problems were a multistep method would need to be used. However, we may highlight the following remarks.

First, we contribute to the intuitive idea that the ODE solver approximation error should be put in the perspective of the observational error. Bayes Factors, and the Bayesian model comparison machinery, can be used as an appropriate measure of the solver accuracy, precisely in the perspective of the observational error considered in the model. Result 1 establishes a consistency in order accuracy for the solver and for the posterior distribution, considering BF's. As a consequence, numerical solver precision may be viewed in this perspective and not solely as a black box regressor. As far as the main aim is to make inference on parameters, there is no need to use to highest precision if the data are

(a)

(b)

(c)
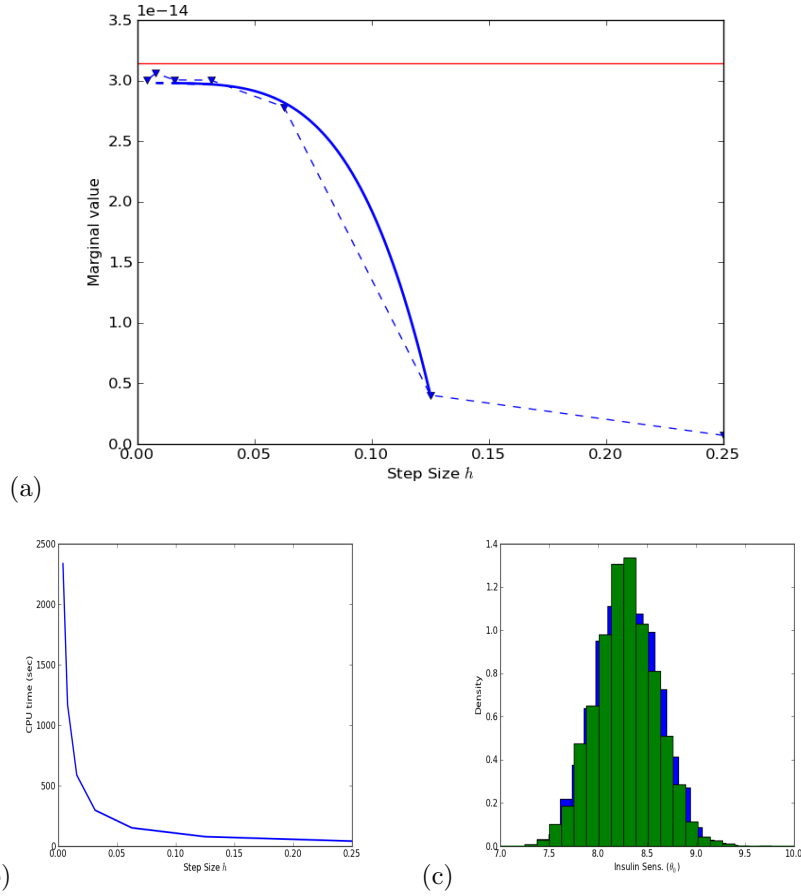
Figure 6: Bayes Factors study for the Diabetes minimal model. An order 4 Runge-Kutta solver was used to produce marginal values $P_{\mathbf{Y}}^h(\mathbf{Y})$ for step sizes as show in (a) and their corresponding CPU times are depicted in (b). The red line in (a) is the numerical integration approximation of $P_{\mathbf{Y}}^h(\mathbf{Y})$ using step size $0.25 \cdot 2^{-7}$ (smallest step size used) while the triangles are Monte Carlo estimates performed as in (13); these seem to slightly underestimate the former. The solid blue line is a regression model $a + bh^4$ estimate using step sizes marginal estimates from $0.25 \cdot 2^{-1}$ to $0.25 \cdot 2^{-4}$ only. In (c) we compare the resulting posterior with step size $0.25 \cdot 2^{-3}$ and $0.25 \cdot 2^{-7}$ showing basically no difference and resulting in a near 90% reduction in CPU evaluation time.

24

contaminated by a non-neglectable quantity of noise. In a domain where the computational time is important, we have proved that considerable time savings can be done, only by using a reasonable step size in the solver.

Secondly, we show how the BF may be approximated even in this scenario where the exact model is not available. This result is of particular interest, since it allows to compare the accuaracy of our approximate posterior without being able to work on the theoretical model directly. The computation of marginal likelihoods is an important topic in the Bayesian literature. In this paper, we propose the use of the Gelfand and Dey's estimator, which has the great advantage of not requiring any additional numerical evaluation of the differential system, after the MCMC was performed. However, we are aware that the Gelfand and Dey's estimator may be highly unstable when the dimension of the parameters increases. The use of a Kernel Density Estimate weighting function in (13) can help to stabilize the estimate but is not a universal solution. If the dimension of the parameters increases, other strategies should be considered, still keeping in mind that any additional numerical evaluation of the ODE system may have a considerable computational cost. Our results would also need to be stated for multiple dimension observation functions f; we leave these considerations for future research.

7 Acknowledgments

References

Atchadé, Y. and J. Rosenthal (2005). On adaptive markov chain monte carlo algorithm. *BERNOULLI*, 815–828.

Cai, C., A. Mohammad-Djafari, S. Legoupil, and T. Rodet (2011). Bayesian data fusion and inversion in x-ray multi-energy computed tomography. In *Proceedings - International Conference on Image Processing, ICIP*, pp. 1377–1380.

Calvetti, D., R. K. Dash, E. Somersalo, and M. E. Cabrera (2006). Local regularization method applied to estimating oxygen consumption during muscle activities. *Inverse Problems 22*(1), 229–243. Cited By (since 1996): 4.

Cao, Y. and L. Petzold (2004). A posteriori error estimation and global error control for ordinary differential equations by the adjoint method. *SIAM Journal on Scientific Computing 26*(2), 359–374.

Capistrán, M., J. Christen, and Velasco-Hernández (2012). Towards uncertainty quantification and inference in the stochastic sir epidemic model. *Mathematical Biosciences 240*(2), 250–259.

Chama, Z., B. Mansouri, M. Anani, and A. Mohammad-Djafari (2012). Image recovery from fourier domain measurements via classification using bayesian approach and total variation regularization. *AEU - International Journal of Electronics and Communications 66*(11), 897–902.

Chen, M. and Q. Shao (1997). On monte carlo methods for estimating ratios of normalizing constants. *The Annals of Statistics 25*(4), 1563–1594.

Christen, J. and C. Fox (2005). Mcmc using an approximation. *Journal of Computer and Graphical Statistics 14*(4), 795–810.

Christen, J. and C. Fox (2010). A general purpose sampling algorithm for continuous distributions (the t-walk). *Bayesian Analysis 5*(2), 263–282.

Cotter, S., M. Dashti, and A. Stuart (2010). Approximation of bayesian inverse problems. *SIAM Journal of Numerical Analysis 48*, 322–345.

Cui, T., C. Fox, and M. J. O'Sullivan (2011). Bayesian calibration of a large-scale geothermal reservoir model by a new adaptive delayed acceptance metropolis hastings algorithm. *Water Resources Research 47*(10). Cited By (since 1996): 1.

Donnet, S. and A. Samson (2007). Estimation of parameters in missing data models defined by differential equations. *J. Statist. Plann. Inference 137*(9), 2815–2831.

Fall, M. D., E. Barat, C. Comtat, T. Dautremer, T. Montagu, and A. Mohammad-Djafari (2011). A discrete-continuous bayesian model for emission tomography. In *Proceedings - International Conference on Image Processing, ICIP*, pp. 1373–1376.

Fox, C., M. Palm, and G. Nicholls (1999). Efficient, exact pde solutions for mcmc. In *Proceedings of SPIE - The International Society for Optical Engineering*, Volume 3816, pp. 23–30.

Gelfand, A. E. and D. K. Dey (1994). Bayesian model choice: asymptotics and exact calculations. *J. Roy. Statist. Soc. B 56*, 501514.

Gutenkunst, R. N., J. J. Waterfall, F. P. Casey, K. S. Brown, C. R. Myers, and J. P. Sethna (2007). Universally sloppy parameter sensitivities in systems biology models. *PLoS computational biology 3*(10), e189.

Haario, H., E. Saksman, and J. Tamminen (1998). An adaptive metropolis algorithm. *Bernoulli 7*, 223–242.

Han, C. and B. P. Carlin (2001). Markov chain Monte Carlo methods for computing Bayes factors: A comparative review. *J. Amer. Statist. Assoc 96*, 11221132.

Hazelton, M. L. (2010). Bayesian inference for network-based models with a linear inverse structure. *Transportation Research Part B: Methodological 44*(5), 674–685. Cited By (since 1996): 2.

Hoeting, J. A., D. Madigan, A. E. Raftery, and C. T. Volinsky (1999). Bayesian model averaging: A tutorial. *Statistical science 14*(4), 382–401.

Iserles, A. (1996). *A first course in the numerical analysis of differential equations.* Number 15. Cambridge University Press.

Kaipio, J. P. and C. Fox (2011). The bayesian framework for inverse problems in heat transfer. *Heat Transfer Engineering 32*(9), 718–753. Cited By (since 1996): 5.

Kaipio, J. P. and E. Somersalo (2005). *Statistical and Computational Inverse Problems.* Applied Mathematical Sciences. Springer Science+Business Media, Incorporated.

Keats, A., E. Yee, and F. . Lien (2010). Information-driven receptor placement for contaminant source determination. *Environmental Modelling and Software 25*(9), 1000–1013. Cited By (since 1996): 7.

Kolehmainen, V., A. Vanne, S. Siltanen, S. Järvenpää, J. P. Kaipio, M. Lassas, and M. Kalke (2007). Bayesian inversion method for 3d dental x-ray imaging. *Elektrotechnik und Informationstechnik 124*(7-8), 248–253. Cited By (since 1996): 2.

Kozawa, S., T. Takenouchi, and K. Ikeda (2012). Subsurface imaging for anti-personal mine detection by bayesian super-resolution with a smooth-gap prior. *Artificial Life and Robotics 16*(4), 478–481.

Lambert, J. D. (1991). *Numerical methods for ordinary differential systems: the initial value problem.* John Wiley & Sons, Inc.

Lang, J. and J. G. Verwer (2007). On global error estimation and control for initial value problems. *SIAM Journal on Scientific Computing 29*(4), 1460–1475.

Mohammad-Djafari, A. (2006). Bayesian inference for inverse problems in signal and image processing and applications. *International Journal of Imaging Systems and Technology 16*(5), 209–214.

Nissinen, A., V. P. Kolehmainen, and J. P. Kaipio (2011). Compensation of modelling errors due to unknown domain boundary in electrical impedance tomography. *IEEE Transactions on Medical Imaging 30*(2), 231–242. Cited By (since 1996): 4.

Quarteroni, A., R. Sacco, and F. Saleri (2007). *Numerical mathematics*, Volume 37. Springer.

Robert, C. and G. Casella (2004). *Monte Carlo Statistical Methods*. Springer.

Schwab, C. and A. M. Stuart (2012). Sparse deterministic approximation of bayesian inverse problems. *Inverse Problems 28*(4).

Somersalo, E., A. Voutilainen, and J. P. Kaipio (2003). Non-stationary magnetoencephalography by bayesian filtering of dipole models. *Inverse Problems 19*(5), 1047–1063. Cited By (since 1996): 24.

Vehtari, A. and J. Lampinen (2000). Bayesian mlp neural networks for image analysis. *Pattern Recognition Letters 21*(13-14), 1183–1191. Cited By (since 1996): 13.

Wan, J. and N. Zabaras (2011). A bayesian approach to multiscale inverse problems using the sequential monte carlo method. *Inverse Problems 27*(10).

Watzenig, D. and C. Fox (2009). A review of statistical modelling and inference for electrical capacitance tomography. *Measurement Science and Technology 20*(5). Cited By (since 1996): 13.

Woodbury, A. D. (2011). Minimum relative entropy, bayes and kapur. *Geophysical Journal International 185*(1), 181–189. Cited By (since 1996): 1.

Zhu, S., P. You, H. Wang, X. Li, and A. Mohammad-Djafari (2011). Recognition-oriented bayesian sar imaging. In *2011 3rd International Asia-Pacific Conference on Synthetic Aperture Radar, APSAR 2011*, pp. 153–156.